Biosensors and Bioelectronics 234 (2023) 115356

Contents lists available at ScienceDirect

Biosensors and Bioelectronics

journal homepage: www.elsevier.com/locate/bios

Size-classified monitoring of ATP bioluminescence for rapid assessment of biological distribution in airborne particulates

Jaeho Oh [a], Jisoo Choi [a], Milad Massoudifarid [a], Ja Young Park [b], Jungho Hwang [a,*], Jiseok Lim [c,**], Jeong Hoon Byeon [c,***]

[a] School of Mechanical Engineering, Yonsei University, Seoul, 03722, Republic of Korea
[b] Gyeongsangbuk-Do Institute of Health and Environment, Yeongcheon, 38874, Republic of Korea
[c] School of Mechanical Engineering, Yeungnam University, Gyeongsan, 38541, Republic of Korea

ARTICLE INFO

Keywords:
Bioaerosols
Adenosine triphosphate bioluminescence
Airborne particulate matter
Size-classified
Specific bioluminescence

ABSTRACT

The COVID-19 pandemic ignited massive research into the rapid detection of bioaerosols. In particular, nanotechnology-based detection strategies are proposed as alternatives because of issues in bioaerosol enrichment and lead time for molecular diagnostics; however, the practical implementation of such techniques is still unclear due to obstacles regarding the large research and development effort and investment for the validation. The use of adenosine triphosphate (ATP) bioluminescence (expressed as relative luminescence unit (RLU) per unit volume of air) of airborne particulate matter (PM) to determine the bacterial population as a representative of the total bioaerosols (viruses, bacteria, and fungi) has been raised frequently because of the high reponse speed, resolution, and compatibility with culture-based bioaerosol monitoring. On the other hand, additional engineering attempts are required to confer significance because of the size-classified (bioluminescence for different PM sizes) and specific (bioluminescence per unit PM mass) biological risks of air for providing proper interventions in the case of airborne transmission. In this study, disc-type impactors to cut-off aerosols larger than 1 μm, 2.5 μm, and 10 μm were designed and constructed to collect PM1, PM2.5, and PM10 on sampling swabs. This engineering enabled reliable size-classified bioluminescence signals using a commercial ATP luminometer after just 5 min of air intake. The simultaneous operations of a six-stage Andersen impactor and optical PM spectrometers were conducted to determine the correlations between the resulting RLU and colony forming unit (CFU; from the Andersen impactor) or PM mass concentration (deriving specific bioluminescence).

1. Introduction

The coronavirus disease 2019 (COVID-19) pandemic has highlighted the importance of developing rapid detection systems for bioaerosols (Matavulj et al., 2022; Qiu et al., 2022; Zhu et al., 2022). Because of the limitations of a large volume of air sampling and the tedious procedure of molecular diagnostics (*e.g.*, polymerase chain reaction (PCR)), various nanotechnology-based real-time detection technologies have been proposed (Addor et al., 2022; Agranovski and Usachev, 2021; Priyamvada et al., 2021); however, they still require numerous research and development efforts and investment for validation and practical implementation. Moreover, the deployment of relevant experts may be a prerequisite utilizing and maintaining the nanotechnology-based detection systems for actual situations, impeding the general use of the detection systems for pandemics from the airborne transmission of respiratory pathogens (Kathiriya et al., 2021; Tahir et al., 2020; Xu et al., 2022a; Yang et al., 2022).

Considering the coexistence of viruses and bacteria in infectious aerosols (Fernandez et al., 2018; Jayaweera et al., 2020; Stiti et al., 2022), including the airborne microbial ecosystem (Chen et al., 2021; Flies et al., 2020; Habibi et al., 2022; Perrone et al., 2022), the approach of indicating the biological hazard of the air from the bacterial population in bioaerosols (*i.e.*, airborne viruses, bacteria, and fungi) as an indicator can provide a representative measure and offer a workable protocol for rapid implementation using a generalized detection system (*e.g.*, agar-based air sampling and incubation (longer than 24 h at the

* Corresponding author.
** Corresponding author.
*** Corresponding author.
E-mail addresses: hwangjh@yonsei.ac.kr (J. Hwang), jlim@yu.ac.kr (J. Lim), postjb@yu.ac.kr (J.H. Byeon).

https://doi.org/10.1016/j.bios.2023.115356
Received 24 January 2023; Received in revised form 11 April 2023; Accepted 26 April 2023
Available online 28 April 2023

very least) to express as colony forming unit (CFU) per unit volume of air) (Marcovecchio and Perrino, 2020; Rocha-Melogno et al., 2020). The countries in North America, Europe, and East Asia selected "CFU/m^3" as a quantitative guideline or standard for bioaerosols to represent airborne microbial cleanliness or contamination (Burge et al., 1989; HKEPD, 2019; Korea Ministry of Environment, 2021; Rao et al., 1996). A single- or six-stage impactor containing agar collection plates was usually used to sample and incubate viable airborne particulates for the determination of CFU/m^3 (Ali et al., 2022; Yan et al., 2022; Zhao et al., 2022).

Based on the rapid reaction kinetics and high resolution, adenosine triphosphate (ATP) bioluminescence (expressing as relative luminescence unit (RLU) per unit volume of air) has recently been introduced as a rapid detection protocol (the fastest was approximately 3 min) to quantify a relative bacterial population in the air (Calabretta et al., 2020; Cho et al., 2020; Fang et al., 2016; Kim et al., 2019; Park et al., 2014, 2015; Yoon et al., 2010). The correlation between CFU/m^3 and RLU/m^3 can be made reliable (exhibiting higher R^2 value (a statistical measure representing the proportion of the variance)) by increasing the number of detection data (Heo et al., 2021). Nevertheless, there were issues in lead time and viability but a nonculturable state to obtain the correlation (Jiang et al., 2022). On the other hand, ATP bioluminescence analysis still has limitations in providing meaningful information other than high and low bacterial populations in the air. The size-segregated bioluminescence, including the biological fraction of airborne particulate matter (PM), needs to be presented to provide proper interventions from the bioluminescence measurements because the airborne transmission path may vary according to the sizes of respiratory bioaerosols (Liu et al., 2022; Pertegal et al., 2023; Xu et al., 2021, 2022b; Zhang et al., 2022).

As a timely, affordable, implementable, and extendable manner, this study highlights the need to seek other approaches to develop a promptly realizable track of the detection for providing proper intervention measures in pandemics, including analogous environmentally and occupationally transmitted settings. From the perspective of re-creating detection strategies using existing principles and devices, this study attempted to recombine technically proven devices (ATP luminometer and airborne PM monitor) and components (inertial impactor and ultrasonic humidifier) to generate size-classified (biological populations for different PM sizes) and specific (biological fraction per unit mass of PM) bioluminescence without a technical delay. Through this recombination, ATP bioluminescence detection of size-classified PMs was conducted simultaneously with optical PM monitoring to provide the size distribution of bioluminescence and bioluminescence per unit PM mass for indoor environments through 5 min permeation of the air (25 L per each size) through the sampling swabs. In particular, disc-type inertial impactors were designed and installed in front of the swabs to classify PM1 (airborne particulates $\leq$1 μm in diameter), PM2.5 (particulates $\leq$2.5 μm), and PM10 (particulates $\leq$10 μm) to be collected on the surfaces of individual swabs for acquiring size-segregated ATP bioluminescence. The PM collection in the absence of the impactors was also conducted to obtain the bioluminescence of the total suspended particle (TSP). The corresponding CFU/m^3 was obtained using a six-stage Andersen impactor to examine the correlations between the RLU/m^3 and CFU/m^3 for PM1, PM2.5, PM10, and TSP. The average mass concentrations (μg/m^3) of the PMs and TSP were obtained simultaneously by portable optical spectrometers during swab collection. The size-classified RLU/m^3 data were eventually divided by the mass concentrations of the PMs to derive RLU/μg levels that demonstrate biological significance on the sizes of airborne particulates. Furthermore, species analyses of the colonies on agar plates after incubation were carried out to identify the signal sources of the size-classified bioluminescence by matrix-assisted laser desorption/ionization time-of-flight mass spectrometry (MALDI-ToF MS).

2. Experimental

2.1. ATP bioluminescence detection system

As shown in Fig. 1A, airborne PMs were collected on sampling swabs in a handheld prototype, where a disc-type inertial impactor was installed in front of the swab (immediately after the air inlet). Three cut-off diameters for the impactor construction were selected to classify PM sizes of 1, 2.5, and 10 μm. The inset table in Fig. 1A represents the main parameters to design the impactors, and the theoretical approach to derive the diameters of the nozzles is described in Supporting Information (**Eqs. S1-S6** and Fig. S1). The cut-off diameters were validated before the ATP bioluminescence detection (Fig. S2), and the resulting values were 1.14, 2.58, and 9.75 μm for the size-classification of PM1, PM2.5, and PM10, respectively (**Eq. S7** and Fig. S3). Airborne PMs passed through the impactors when the motor was turned on to intake air (5 L/min, regulated by the flowmeter), where PMs larger than 1, 2.5, or 10 μm in diameter were collected on an impaction plate to be removed. The size-classified PM-laden airflow was then injected into a swab (UXL100, 3M, USA) for 5 min to collect the PM on the swab surface. For the last 30 s of the intake, bacterial lysis buffer (diluted 1000 times; bacterial protein extraction reagent (B-PER™), ThermoFisher Scientific, USA) droplets were produced using an ultrasonic humidifier (installed between the impactor and swab loading column; G5, Highon, Korea) to be co-collected on the surface of the swab for ATP extraction from the PM. A silica chamber next to the swab-loading column was used to eliminate the water from the airflow. After PM collection (including lysis buffer droplets), the swab was immersed in a cuvette containing reagents for the luciferin-luciferase reaction under vortex mixing for 5 s. As shown in Fig. 1B, ATP bioluminescence from the reaction was obtained using a photomultiplier tube-type luminometer (Clean-Trace LM1, 3M, USA), as shown in Supplementary Video Clip.

Supplementary video related to this article can be found at https://doi.org/10.1016/j.bios.2023.115356

2.2. RLU-CFU from lab test

Staphylococcus aureus (*S. aureus*; Korean Collection for Type Cultures (KCTC) 1621) was used as test bacteria (Supporting Information, Fig. S4) because its presence in indoor as a component of airborne dust (White et al., 2020). The prepared bacterial suspension was aerosolized using a collison-type atomizer (9302, TSI, USA) in the presence of a particle-free compressed air supply (CAS-01, HCTm, Korea). The flowrate of the air (set at 2 L/min) was regulated using a mass flow controller (3660, KOFLOC, Japan). The droplets containing *S. aureus* from the atomizer were passed through a diffusion dryer to eliminate moisture to form bioaerosols. The bioaerosols were then diluted with particle-free air after charge neutralization using a soft X-ray charger (4530, HCT, Korea) to realize an electrostatically neutral state. The resulting bioaerosol-laden air entered the developed sampler at a flowrate of 5 L/min to be collected on the sampling swabs. The optimal duration (30 s) of the lysis buffer droplet supply was determined by scanning electron microscopy (SEM; 7800F, JEOL, Japan) of *S. aureus* on the swab (collected for 2 min) after exposure to the droplets with different durations (10-50 s), as shown in Fig. S5A. The number concentration of airborne *S. aureus* was monitored using an aerodynamic particle sizer (APS; 3321, TSI, USA) after the injection of charge-neutralized *S. aureus*-laden airflow into a square duct (4 × 4 cm^2), as shown in Fig. S5B. The levels of CFU/m^3 for comparison were determined by the simultaneous delivery of the *S. aureus*-laden flow (28.3 (2.0 for bioaerosol flow + 26.3 for dilution flow) L/min for 2 min) to a six-stage Andersen impactor (TE-10-880, Tisch Environmental, USA) containing agar (tryptic soy) plates based on the standard testing method (ES 0271. 1d) notified by the Ministry of Environment of Korea. The *S. aureus*-exposed agar plates were then placed in an incubator (VS-1203P4S, VISIONBIONEX, Korea) for 24 h at 37°C, and the number

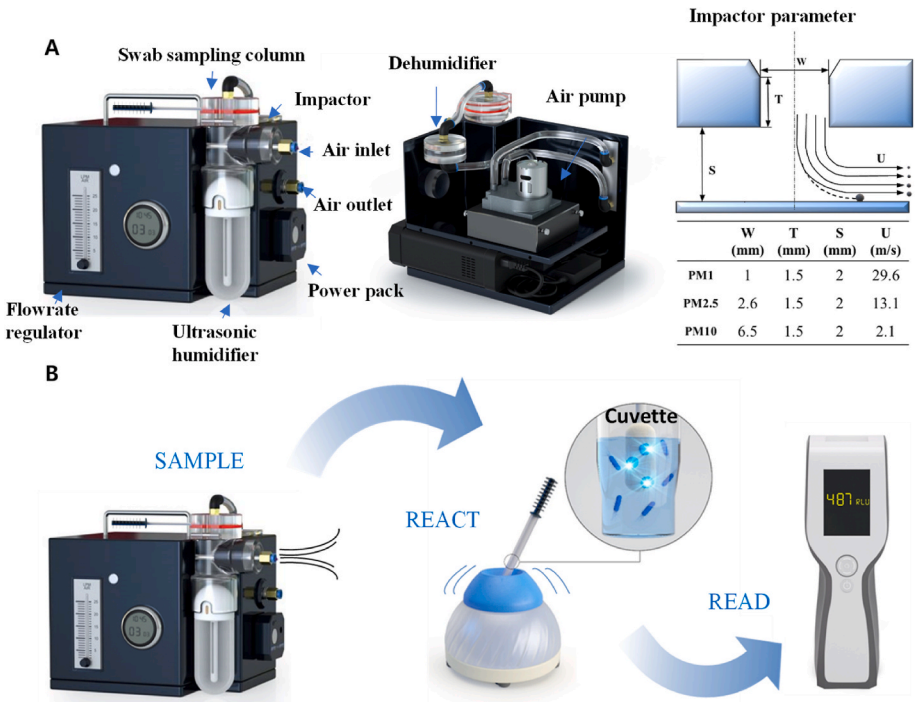

	W (mm)	T (mm)	S (mm)	U (m/s)
PM1	1	1.5	2	29.6
PM2.5	2.6	1.5	2	13.1
PM10	6.5	1.5	2	2.1

Fig. 1. Illustration of the sampling platform for detecting the size-classified ATP bioluminescence in the airborne PMs. (A) Major components of the platform and design parameters to construct inertial impactors are to be installed in front of the swab sampling column for classifying PM1, PM2.5, and PM10. (B) The protocol to read ATP bioluminescence of the PMs as RLU. The PMs after the impactors were collected on the surfaces of the individual swabs to be immersed in cuvettes for luciferin-luciferase reaction under vortexing to generate bioluminescence. The luminescence intensity (*i.e.*, RLU) was acquired using a commercially available luminometer to secure the size-classified microbial population in air. The RLU/m^3 values were estimated by dividing the obtained RLU by the sampled air volume.

of colonies was counted to estimate CFU/m^3.

For analogous analysis in the qualified testing agency (Gyeongbuk Technopark, Korea), *S. aureus* suspension (1×10^3, 2×10^3, or 4×10^3 CFU/mL) was aerosolized for 1 min with a flowrate of 1200 cm^3/h using a commercial humidifier (DEH-R135A, Daewoo Electronics, Korea) to be suspended in a test chamber (2 m^3) with a fixed relative humidity (40%). After securing uniform distribution in the chamber using a circulating fan, the part of the *S. aureus*-laden air was simultaneously sampled by a viable active sampler (MAS-100 eco, Merck, Germany) and the developed prototype for comparison. After incubation (24 h at 37 °C) of agar plates installed in the viable sampler, the correlation between the CFU/m^3 and RLU/m^3 was analyzed.

2.3. RLU-CFU from field test

The field monitoring was carried out in three different indoor environment settings for public education (elementary, middle, and high school class rooms), public transportation (airport and subway and train stations), and other purposes (general hospital lobby, chapel). The ranges of temperatures and relative humidity were 22.5-25.9 °C and 47.0-71.7%, respectively. The CFU/m^3 levels for TSP (without impactors) were determined using a single-stage agar plate-inserted sampler (Spin Air, IUL, Spain). In contrast, average TSP (μg/m^3) levels were obtained using an optical TSP monitor (PMM-304, APM Engineering, Korea), as shown in Fig. S6A. Similar CFU/m^3 and PM mass concentration data for size-classified configurations were obtained using the six-stage Andersen impactor and optical PM spectrometer (Innoair-315, Innociple, Korea), respectively (Fig. S6B). A part of colonies after growth in the incubator was isolated for species analyses using Biotyper 3.0 microbial identification system (LRF20, Bruker Daltonics, Germany) coupled with a MALDI-ToF MS system (Supporting Information; Figs. S7 and S8).

Plots containing RLU/m^3 and CFU/m^3 data were generated using mean ± standard deviation values from at least three independent experiments for each sampling point.

3. Results and discussion

3.1. Effect of pre-lysis

The pre-lysis of biological particles in the collected PMs on the swab for a few minutes before immersing them in a cuvette was reported as a key procedure for the luciferin-luciferase reaction to generate readable bioluminescence signals (Kim et al., 2019). To determine the optimal duration of the pre-lysis, the diluted lysis buffer droplets generated by an ultrasonic humidifier were supplied to aerosolized *S. aureus* collected swabs. The morphological changes in *S. aureus* upon exposure to the droplets with predetermined supply times (10-50 s) were observed by SEM, as shown in Fig. 2. The spherical shape with a smooth surface of the untreated *S. aureus* was melted and distorted by increasing the droplet supply time, and these collapsed completely after 30 s of supply. No significant alterations in shape were observed by prolonging the droplet supply. Hence, 30 s may be practical to extract both intracellular and extracellular ATP from the collected bacteria for achieving rapid detection with sufficient bioluminescence signal strength.

3.2. Correlations between RLU/m^3 and CFU/m^3 at laboratory-controlled conditions

Based on the selected duration of the lysis droplet supply, co-plotting of the ATP bioluminescence and number of *S. aureus* colonies (or number concentration of aerosolized *S. aureus* obtained by APS) per 1 m^3 of air was conducted to identify the correlations, as represented as R^2. The RLU/m^3 were proportional to the counted colonies (Fig. 3A) and aerosol *S. aureus* numbers (Fig. 3B), where the R^2 values of the plots were 0.938 and 0.951, respectively. This suggests that the developed protocol based on a 30 s duration for the lysis droplet supply effectively acquired reliable bioluminescence signals for determining bioaerosol concentrations without a tedious cell culture procedure. The reliability of the developed platform was examined further by one (Gyeongbuk Technopark) of the qualified testing agencies in South Korea for bioaerosol detection, which has a 2 m^3 test chamber to aerosolize and sample *S. aureus* for incubation and subsequent colony counting. Fig. 3C shows the plot reported by the agency, which was consistent (R^2 = 0.939) with those from the

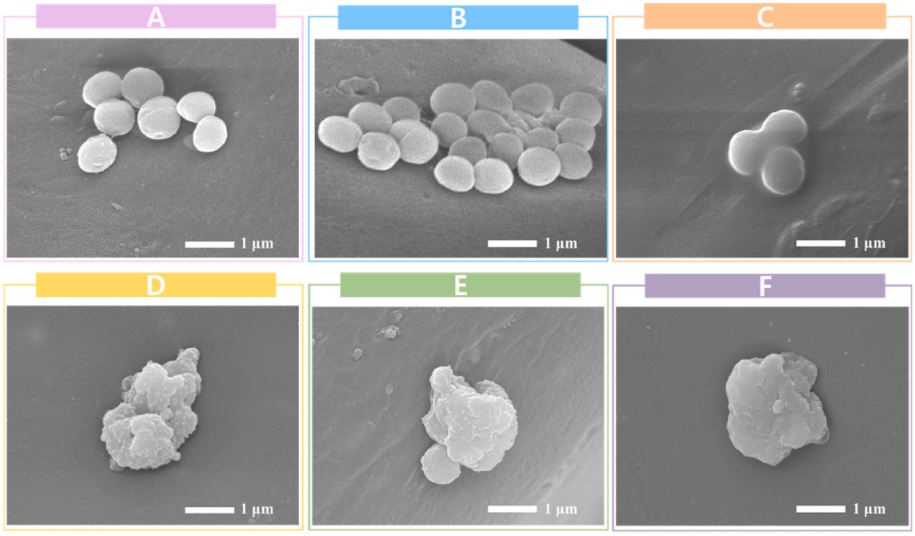

Fig. 2. Morphologies of aerosol *S. aureus* collected on sampling swabs. The SEM observation was conducted to obtain images for untreated (A), 10 s (B), 20 s (C), 30 s (D), 40 s (E), and 50 s (F) supply of the diluted lysis buffer droplets on the *S. aureus* collected swab surfaces.

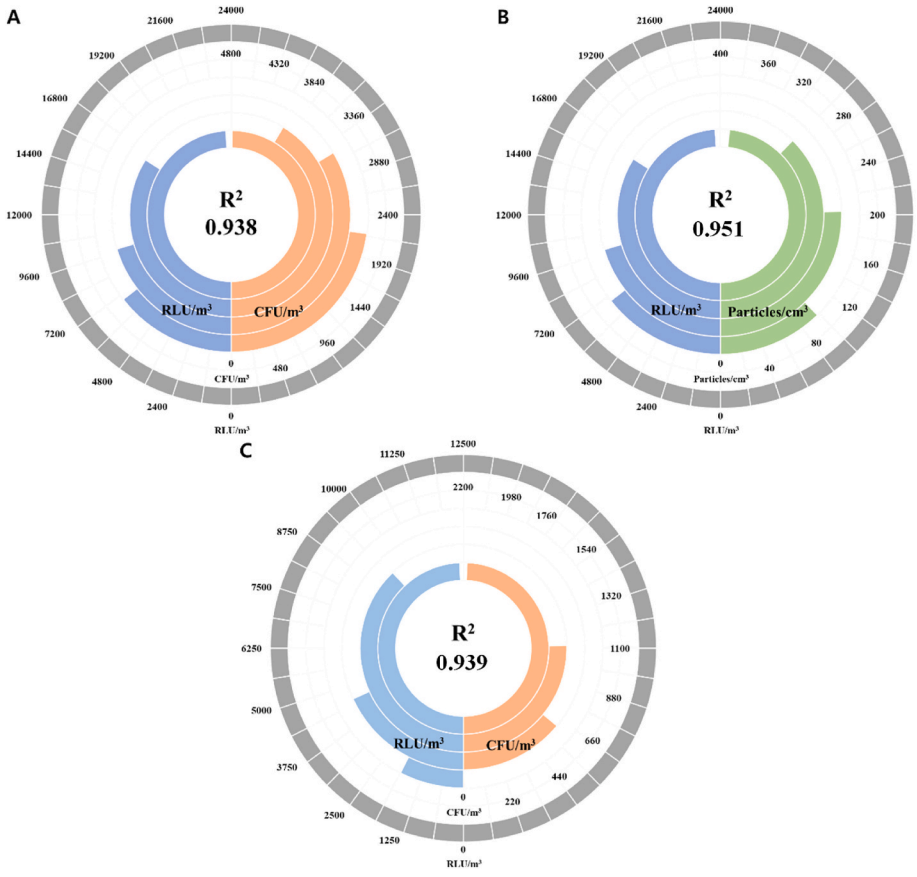

Fig. 3. Plots to assess the correlations between RLU/m^3 and CFU/m^3 (or particle number concentration, particles/cm^3) at laboratory-controlled conditions. (A, B) RLU/m^3-CFU/m^3 (or particles/cm^3 obtained APS) plot for aerosolized *S. aureus* to identify the correlation between the developed platform and culture-based colony counting. (C) RLU/m^3-CFU/m^3 plot from the tests by the qualified testing agency (Certificate No. 22-0205; Gyeongbuk Technopark, Korea) through the suspension of *S. aureus* with different predetermined concentrations in the air of a 2 m^3 chamber.

laboratory tests, warranting further investigation for field tests.

3.3. Correlations between RLU/m^3 and CFU/m^3 at field testing conditions

The developed platform for realistic settings was validated by scouting different public indoor places to operate the developed platform with a single- or six-stage impactor to plot RLU/m^3-CFU/m^3. The resulting plot (Fig. 4) exhibited linearity with $R^2 \geq 0.9$. The correlation between the RLU/m^3 and CFU/m^3 was comparable to that from the controlled environment (Fig. 3), even though bioaerosols usually co-existed with non-biological PMs (*e.g.*, dust) for natural indoor environments (Bowers et al., 2013; Li et al., 2017; Wang et al., 2010), unlike the laboratory-controlled conditions. Because of diversity of microbial species in the air, sampling and comparison to ensure reliable correlation between the RLU/m^3 and CFU/m^3 were conducted more than 600 times referring to our previous study for the statistical convergence (Kim et al., 2019), even for realistic settings. The results also suggest that the pre-lysis can establish consistent performance across bare and

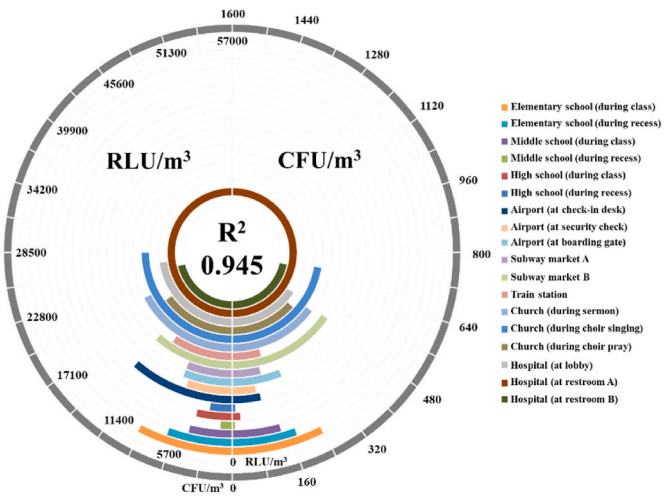

Fig. 4. RLU/m^3-CFU/m^3 plot from field tests at various public indoor facilities. The tests were conducted with the consent of the organizations and under the observation of the person in charge. The measurements were repeated more than three times at each point.

dust-incorporated bioaerosols, but it is unclear if ATP in airborne PMs had been completely extracted through the lysis droplet supply because PMs in indoor environments also include fungal spores (Venkateswaran et al., 2003). This was also related to the wetting of the swabs by the lysis droplet supply that compensates for the bioluminescence signal irregularities during the luciferin-luciferase reaction from the diversity of PM composition in the absence of pre-lysis. The selectivities (the slope (a) in the linear ($y = ax + b$) trend line of RLU/m^3-CFU/m^3 plot) with pre-lysis were more than 1.4 times greater than those without pre-lysis for the comparison at whole sampling points, supporting that pre-lysis is a viable pretreatment for reliable acquisition of the bioluminescence signals, even with non-biological PMs. In addition, the broad distributions of RLU/m^3 and CFU/m^3 values varied according to the number and activity of occupants, including the situation of air conditioning and cleaning. The developed platform may cover various levels of air quality in terms of biological risk, according to the high correlation between the RLU/m^3 and CFU/m^3 for the broad range of field tests.

3.4. *Size-classified ATP bioluminescence and colony counting results at field testing conditions*

The data for size-classified bioluminescence and colony count were

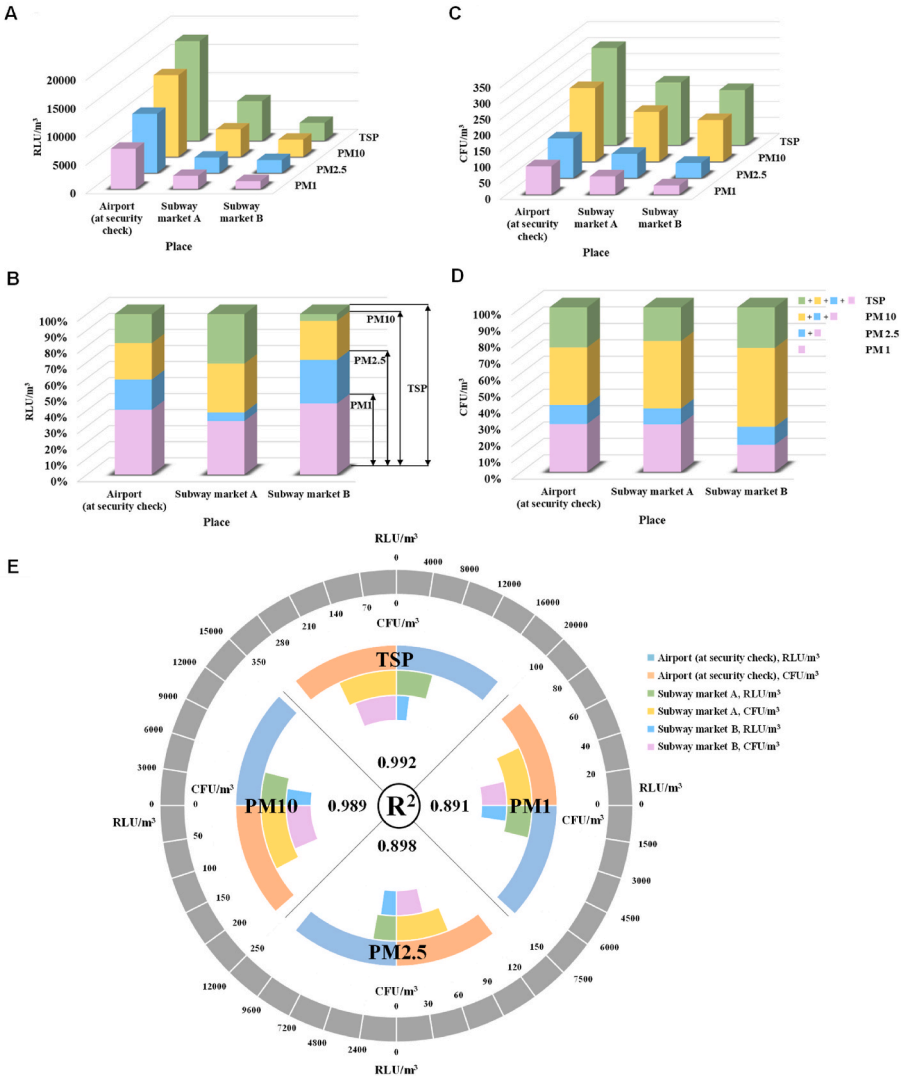

Fig. 5. Size-classified ATP bioluminescence and colony counting results at the selected points (airport and subway markets) for the field tests. (A, B) Size distributions and relative fractions of RLU/m^3 for each PM section. (C, D) Analogous data based on CFU/m^3 for each PM section. (E) R^2 values for PM1, PM2.5, PM10, and TSP to determine size-classified correlations between the RLU/m^3 and CFU/m^3.

acquired at several points for the field tests, as shown in Fig. 5A and B. The RLU/m^3 and CFU/m^3 values increased cumulatively as the PM size increased. Based on the results consistent with physical phenomena, the microbial population could be segregated stoichiometrically, as shown in Fig. 5C and D, providing the population distribution with different PM sizes. Through size-classification, it was possible to identify which PM sections have dominant distributions of bioaerosols. Furthermore, there were no significant differences in the distribution between the ATP bioluminescence and culture-based colony measurements. This observation suggests that reliable data for bioaerosol size distribution can be secured through the size-classified detections of the bioluminescence of PMs in a few minutes without waiting for colony growth. The RLU/m^3-CFU/m^3 correlation exhibited $R^2 \geq 0.89$, even for the size-classified configurations (Fig. 5E), proving that the integration of a lysis droplet supply, inertial impaction, and luciferin-luciferase reaction is a viable option for the rapid analysis of bioaerosol size distribution.

3.5. PM and size-classified specific bioluminescence results at field testing conditions

The specific bioluminescence (bioluminescence per unit mass of PM) data were determined by dividing RLU/m^3 by PM mass concentration (μg/m^3) that indicates specific biological risks (RLU/μg). The mass concentrations of each PM section were monitored simultaneously and averaged to take this into computation to estimate the size-classified specific bioluminescence for identical points for the field tests (Fig. 6A and B). Relatively higher (lower) levels correspond to relatively higher (lower, mostly non-biological composition) biological fractions of the PM because of coexistence of bioaerosols and non-biological aerosols in the air. Interestingly, the resulting specific bioluminescence exhibited an opposite trend to the size-classified configuration (Fig. 6C and D). In larger PMs, bioaerosols may mainly exist with non-biological dust particles, whereas, in smaller PMs (*i.e.*, PM1 section), they flew in a nearly bare form. Hence, single particles in the PM1 section may have significantly different compositions (nearly biological or non-biological) from those in larger PMs (a mixture of biological and non-biological). In other words, in the case of bioaerosols in PM1, their surfaces are highly likely to come into unprotected exposure to humans and animals. This suggests that concentrating on removing smaller PMs can more efficiently suppress the direct contact of bare bioaerosols with the bodies that can be infected. Unlike previous studies relevant to the ATP bioluminescence detection of bioaerosols, specific bioluminescence data acquired using the developed platform can show the relative biological risks for different PM sections beyond simply showing a microbial population of the air.

3.6. Species identification results at field testing conditions

The signal sources of the bioluminescence were verified by conducting species analyses using MALDI-ToF MS for the sampled bioaerosols in the selected points (airport and subway markets) for the field tests. As shown in Fig. S9, the microrganisms releasing ATP were diversely distributed (mostly originated from the skin, mouth, nostrils, human hair, and pets) (Acheson et al., 2002; Faridi et al., 2015; Kawatsu et al., 2006) with places and PM sizes while the number of microbial species (nine species were identified) for the airport (at security check) was greater than those of subway markets (seven species). These results suggest that the bioluminescence signals mainly came from human activity despite the diversity, while more bioaerosol species can be found when many people's physical actions are performed simultaneously (walking, talking, taking off clothes, and loading baggage on conveyors) in a confined space. Considering the original dimensions of the listed microorganisms, a smaller PM size means a higher probability that the bioaerosols are floating alone in the air. A larger PM size means that bioaerosols can be attached to non-biological dust, which is consistent with the specific bioluminescence data (Fig. 6C and D). In addition, the site-categorized identification of the bioaerosol species was conducted (Fig. S10), where more species of bioaerosols were observed in transportation facilities than in education and other public ones, supporting the positive correlation between the activities of unspecified individuals and bioaerosol diversity, as shown in Fig. S9. Interestingly, the number of identified species for the airport and hospital was greater than other sites despite their relatively low RLU/m^3 and CFU/m^3 levels because of better ventilating situations (Fig. 4), suggesting that air conditioning and cleaning systems can be effective in reducing the bioaerosol concentration, but further action will be needed to reduce the number of bioaerosol species. As the opposite situation, the lowest number of identified species was observed for the church (the most static of the occupants' activities; equivalent to the less crowded environment) despite its RLU/m^3 and CFU/m^3 levels were similar or higher than those for the airport and hospital (Fig. 4). By incorporation with species identification; however, the size-classified and specific bioluminescence data acquired by the developed platform may also assist in developing an epidemiologic investigation related to bioaerosols.

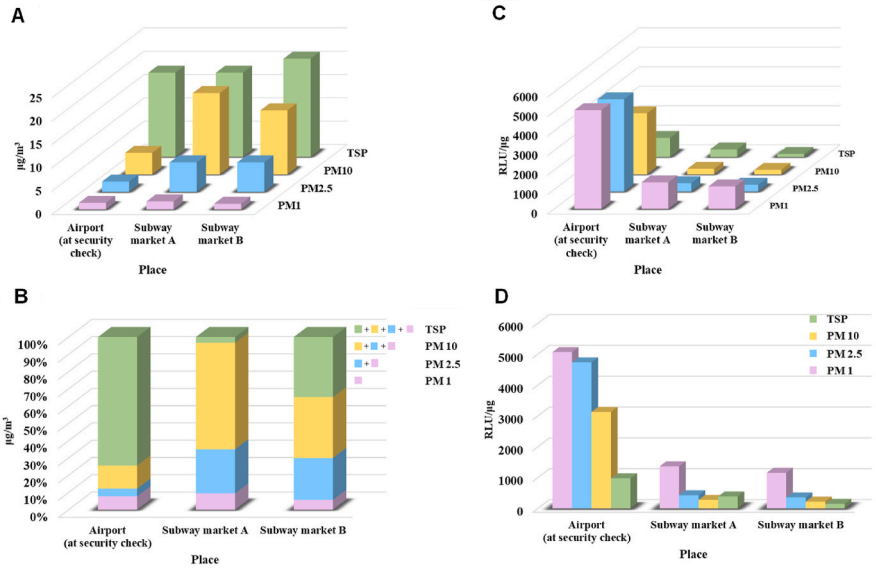

Fig. 6. PM mass concentration (μg/m^3) and size-classified specific bioluminescence (RLU/μg; relative biological risk of each PM section) results at the identical points for the field tests. The size-classified RLU/m^3 levels were individually divided by the mass concentration of each PM or TSP. The average concentrations of PMs and TSP for the sampling period were obtained by commercially available optical spectrometer and TSP monitor, respectively. (A, B) Size distributions and relative fractions of the PMs. (C, D) 3- and 2-axis plots for the size-classified specific bioluminescence.

4. Conclusions

As a rapid implementation methodology, the platform was constructed by recombining a commercially available ATP luminometer and accessories for air sampling and size-classification with no micro/nanofabrication for integrated precision sensors. It was possible to provide which size of airborne PMs has physical dominance and intensity, thereby providing meaningful information for proper intervention measures within minutes. This simple engineering attempt enabled the derivation of reliable data for size-classified microbial populations in the air of different indoor environments for providing proper management strategies for airborne biological risks. The size-classified and specific bioluminescence data were even informative in interpreting species analyses of bioaerosols. The platform developed in this study may be operated even by non-experts as a general-use device to identify bioaerosol exposures in both environmental and occupational settings.

CRediT authorship contribution statement

Jaeho Oh: Experiment, RLU-CFU . **Jisoo Choi:** Experiment and Species identification. **Milad Massoudifarid:** Species identification. **Ja Young Park:** RLU-CFU . **Jungho Hwang:** Conceptualization, Formal analysis, Writing – review & editing, Supervision, Funding acquisition. **Jiseok Lim:** Conceptualization, Formal analysis, Writing – review & editing, Funding acquisition. **Jeong Hoon Byeon:** Conceptualization, Investigation, Formal analysis, Writing – original draft, Writing – review & editing, Data curation, Supervision, Funding acquisition.

Declaration of competing interest

The authors declare that they have no known competing financial interests or personal relationships that could have appeared to influence the work reported in this paper.

Data availability

Data will be made available on request.

Acknowledgements

This work was supported by Korea Environment Industry & Technology Institute (KEITI) through Technology Development Project for Biological Hazards Management in Indoor Air Program, funded by Korea Ministry of Environment (MOE) (2021003370005). This work was also supported by KEITI through Technology Development Project for Biological Hazards Management in Indoor Air Program, funded by MOE (ARQ202101038001). This research was also supported by the National Research Foundation of Korea (NRF) funded by the Ministry of Science, ICT and future Planning (No. 2022R1A2C1009389 and No. 2021R1A6A1A03039493).

Appendix A. Supplementary data

Supplementary data to this article can be found online at https://doi.org/10.1016/j.bios.2023.115356.

References

Acheson, D., Bresee, J.S., Widdowson, M.A., Monroe, S.S., Glass, R.I., 2002. Clin. Infect. Dis. 35, 748–753. https://doi.org/10.1086/342386.

Addor, Y.S., Baumgardner, D., Hughes, D., Newman, N., Jandarov, R., Reponen, T., 2022. Environ. Sci. Process. Impacts 24, 1790–1804. https://doi.org/10.1039/D2EM00177B.

Agranovski, I.E., Usachev, E.V., 2021. Atmos. Environ. 246, 118147 https://doi.org/10.1016/j.atmosenv.2020.118147.

Ali, W., An, D.-z., Yang, Y.-f., Cui, B.-b., Ma, J.-x., Zhu, H., Li, M., Ai, X.-J., Yan, C., 2022. Build. Environ. 221, 109284 https://doi.org/10.1016/j.buildenv.2022.109284.

Bowers, R.M., Clements, N., Emerson, J.B., Wiedinmyer, C., Hannigan, M.P., Fierer, N., 2013. Environ. Sci. Technol. 47, 12097–12106. https://doi.org/10.1021/es402970s.

Burge, H.A., Feeley, J.C., Kreiss, K., Milton, D., Morey, P.R., Otten, J.A., Peterson, K., Tulis, J.J., Tyndall, R., 1989. Guidelines for the assessment of bioaerosols in the indoor environment. In: American Conference of Governmental Industrial Hygienists, 093671283X, 9780936712833.

Calabretta, M.M., Álvarez-Diduk, R., Michelini, E., Roda, A., Merkoçi, A., 2020. Biosens. Bioelectron. 150, 111902 https://doi.org/10.1016/j.bios.2019.111902.

Chen, N.-T., Cheong, N.-S., Lin, C.-Y., Tseng, C.-C., Su, H.-J., 2021. Environ. Pollut. 270, 116231 https://doi.org/10.1016/j.envpol.2020.116231.

Cho, Y.S., Kim, H.R., Ko, H.S., Jeong, S.B., Kim, B.C., Jung, J.H., 2020. ACS Sens. 5, 395–403. https://doi.org/10.1021/acssensors.9b02001.

Fang, W., Liu, C., Yu, F., Liu, Y., Li, Z., Chen, C., Bao, X., Tu, T., 2016. ACS Appl. Mater. Interfaces 8, 20583–20590. https://doi.org/10.1021/acsami.6b05804.

Faridi, S., Hassanvand, M.S., Naddafi, K., Yunesian, M., Nabizadeh, R., Sowlat, M.H., Kashani, H., Gholampour, A., Niazi, S., Zare, A., Nazmara, S., Alimohammadi, M., 2015. Environ. Sci. Pollut. Res. 22, 8190–8200. https://doi.org/10.1007/s11356-014-3944-y.

Fernandez, M.O., Thomas, R.J., Garton, N.J., Hudson, A., Haddrell, A., Reid, J.P., 2018. J. R. Soc. Interface 16, 20180779. https://doi.org/10.1098/rsif.2018.0779.

Flies, E.J., Jones, P., Buettel, J.C., Brook, B.W., 2020. Front. Ecol. Evol. 8, 568902 https://doi.org/10.3389/fevo.2020.568902.

Habibi, N., Uddin, S., Behbehani, M., Salameen, F.A., Razzack, N.A., Zakir, F., Shajan, A., Alam, F., 2022. Front. Microbiol. 13, 955913 https://doi.org/10.3389/fmicb.2022.955913.

Heo, K.J., Ko, H.S., Jeong, S.B., Kim, S.B., Jung, J.H., 2021. Nano Lett. 21, 1017–1024. https://doi.org/10.1021/acs.nanolett.0c04096.

HKEPD (The Hong Kong Environmental Protection Department), 2019. Indoor Air Quality Management Group. Guideline Notes for the Management of Indoor Air Quality in Offices and Public Places. https://www.iaq.gov.hk/wp-content/uploads/2021/04/gn_officeandpublicplace_eng-2019.pdf. (Accessed 6 December 2022).

Jayaweera, M., Perera, H., Gunawardana, B., Manatunge, J., 2020. Environ. Res. 188, 109819 https://doi.org/10.1016/j.envres.2020.109819.

Jiang, G., Ma, J., Wang, C., Wang, Y., Laghari, A.A., 2022. Sci. Total Envion. 832, 155033 https://doi.org/10.1016/j.scitotenv.2022.155033.

Kathiriya, T., Gupta, A., Singh, N.K., 2021. Environ. Technol. Innov. 21, 101287 https://doi.org/10.1016/j.eti.2020.101287.

Kawatsu, K., Ishibashi, M., Tsukamoto, T., 2006. J. Clin. Microbiol. 44, 1821–1827. https://doi.org/10.1128/JCM.44.5.1821-1827.2006.

Kim, H.R., An, S., Hwang, J., Park, J.H., Byeon, J.H., 2019. J. Hazard Mater. 369, 684–690. https://doi.org/10.1016/j.jhazmat.2019.02.088.

Korea Ministry of Environment, 2021. Enforcement Rules of the Domestic Indoor Air Quality Management Act. Ministry of Environment Ordinance No. 918, Annex 2 Maintenance Standards. https://www.law.go.kr/법령/실내공기질관리법시행규칙.

Liu, Z., Wu, M., Cao, H., Liu, H., Wang, H., Lv, J., Rong, R., He, J., 2022. Build. Environ. 225, 109649 https://doi.org/10.1016/j.buildenv.2022.109649.

Li, Y., Lu, R., Li, W., Xie, Z., Song, Y., 2017. J. Aerosol Sci. 106, 83–92. https://doi.org/10.1016/j.jaerosci.2017.01.007.

Marcovecchio, F., Perrino, C., 2020. Chemosphere 264, 128510. https://doi.org/10.1016/j.chemosphere.2020.128510.

Matavulj, P., Cristofori, A., Cristofolini, F., Gottardini, E., Brdar, S., Sikoparija, B., 2022. Sci. Total Environ. 851, 158234 https://doi.org/10.1016/j.scitotenv.2022.158234.

Park, C.W., Park, J.-W., Lee, S.H., Hwang, J., 2014. Biosens. Bioelectron. 52, 379–383. https://doi.org/10.1016/j.bios.2013.09.015.

Park, J.-W., Park, C.W., Lee, S.H., Hwang, J., 2015. PLoS One 10, e0125251. https://doi.org/10.1371/journal.pone.0125251.

Perrone, M.R., Romano, S., de Maria, G., Tundo, P., Bruno, A.N., Tagliaferro, L., Maffia, M., Fragola, M., 2022. Aerobiologia 38, 391–412. https://doi.org/10.1007/s10453-022-09754-7.

Pertegal, V., Lacasa, E., Cañizares, P., Rodrigo, M.A., Sáez, C., 2023. Environ. Res. 216, 114458 https://doi.org/10.1016/j.envres.2022.114458.

Priyamvada, H., Kumaragama, K., Chrzan, A., Athukorala, C., Sur, S., Dhaniyala, S., 2021. Aerosol Sci. Technol. 55, 24–36. https://doi.org/10.1080/02786826.2020.1812503.

Qiu, G., Spillmann, M., Tang, J., Zhao, Y.-B., Tao, Y., Zhang, X., Geschwindner, H., Saleh, L., Zingg, W., Wang, J., 2022. Adv. Sci. https://doi.org/10.1002/advs.202204774.

Rao, C.Y., Burge, H.A., Chang, J.C.S., 1996. J. Air Waste Manage. Assoc. 46, 899–908. https://doi.org/10.1080/10473289.1996.10467526.

Rocha-Melogno, L., Ginn, O., Bailey, E.S., Soria, F., Andrade, M., Bergin, M.H., Brown, J., Gray, G.C., Deshusses, M.A., 2020. Sci. Total Environ. 738, 139495 https://doi.org/10.1016/j.scitotenv.2020.139495.

Stiti, M., Castanet, G., Corber, A., Alden, M., Berrocal, E., 2022. Environ. Res. 204, 112072 https://doi.org/10.1016/j.envres.2021.112072.

Tahir, M.A., Zhang, X., Cheng, H., Xu, D., Feng, Y., Sui, G., Fu, H., Valev, V.K., Zhang, L., Chen, J., 2020. Analyst 145, 277–285. https://doi.org/10.1039/C9AN01715A.

Venkateswaran, K., Hattori, N., la Duc, M.T., Kern, R., 2003. J. Microbiol. Methods 52, 367–377. https://doi.org/10.1016/S0167-7012(02)00192-6.

Wang, Y.-F., Wang, C.-H., Hsu, K.-L., 2010. Atmos. Environ. 44, 4331–4338. https://doi.org/10.1016/j.atmosenv.2010.08.029.

White, J.K., Nielsen, J.L., Larsen, C.M., Madsen, A.M., 2020. Int. J. Hyg Environ. Health 230, 113608. https://doi.org/10.1016/j.ijheh.2020.113608.

Xu, J.C., Wang, C.T., Fu, S.C., Chan, K.C., Chao, C.Y.H., 2021. Aerosol Sci. Technol. 55, 474–485. https://doi.org/10.1080/02786826.2020.1870922.

Xu, J., Wang, C., Fu, S.C., Chao, C.Y.H., 2022b. Indoor Air 32, e12973. https://doi.org/10.1111/ina.12973.

Xu, X., Zhou, W., Xie, C., Zhu, Y., Tang, W., Zhou, X., Xiao, H., 2022a. Sci. Total Environ. 846, 157420 https://doi.org/10.1016/j.scitotenv.2022.157420.
Yan, C., Zhao, X.-y., Luo, X., An, D.-z., Zhu, H., Li, M., Ai, X.-j., Ali, W., 2022. Environ. Sci. Pollut. Res. https://doi.org/10.1007/s11356-022-23621-5.
Yang, J.I.L., Lee, B.G., Park, J.-H., Yeo, M.-K., 2022. Indoor Air 32, e13107. https://doi.org/10.1111/ina.13107.
Yoon, K.Y., Park, C.W., Byeon, J.H., Hwang, J., 2010. Environ. Sci. Technol. 44, 1742–1746. https://doi.org/10.1021/es903437z.
Zhang, Y., Liu, B., Tong, Z., 2022. J. Air Waste Manag. Assoc. https://doi.org/10.1080/10962247.2022.2101566.
Zhao, X.-y., An, D.-z., Liu, M.-l., Ma, J.-x., Ali, W., Zhu, H., Li, M., Ai, X.-j., Nasir, Z.A., Alcega, S.G., Coulon, F., Yan, C., 2022. Sci. Total Environ. 851, 158106 https://doi.org/10.1016/j.scitotenv.2022.158106.
Zhu, X., Zhang, P., Wang, G., Zhu, J., Chen, S., Lu, C., Du, K., Huang, H., 2022. Opt. Eng. 61, 064101 https://doi.org/10.1117/1.OE.61.6.064101.